Seismic Denoising Using Thresholded Adaptive Signal Decomposition

Fangyu Li, University of Oklahoma; Sumit Verma, University of Texas Permian Basin; Pan Deng, University of Houston; Jie Qi, and Kurt J. Marfurt, University of Oklahoma.*

SUMMARY

Noise reduction is critical for structural, stratigraphic, lithological and quantitative interpretation. In the absence of physical insight into its cause and behavior, separating the noise from the underlying signal can be difficult. We construct a noise suppression workflow based on a data-adaptive signal decomposition method (variational mode decomposition). Key to our workflow is to determine which of the generated intrinsic mode functions represent signal and which represent noise. We address this issue by a scaling exponent based on detrended fluctuation analysis. The proposed method shows excellent performance on synthetic and field data, especially when encountering data exhibiting a low signal-to-noise ratio. Laterally continuous events are preserved and steeply dipping coherent events due to aliasing as well as random noise are rejected.

INTRODUCTION

Seismic signal is non-stationary because of complex subsurface structures, random and coherent interferences, as well as acquisition related noises. Denoising is a necessary step to enhance signal-to-noise ratio (SNR) (Li et al., 2014). Methods based on signal decomposition and thresholding scheme show good performance in denoising non-stationary signal (Donoho and Johnstone, 1994; Chkeir et al., 2010). Unlike the popular continuous wavelet transform that consists of applying a suite of stationary filter banks, empirical mode decomposition (EMD) is a data-driven signal decomposition method (Huang et al., 1998). EMD analyzes non-stationary signals and adaptively decomposes signal into oscillatory components called intrinsic mode functions (IMF) plus a residual (Huang et al., 1998). However, EMD has the frequency mixing issue, especially in low SNR situation (Kabir and Shahnaz, 2012). To address this drawback, Dragomiretskiy and Zosso (2014) proposed variational mode decomposition (VMD) to decompose a signal into an ensemble of band-limited IMFs. VMD solves an optimization problem in frequency domain to best isolate different spectral modes. In VMD, low order IMFs represent slow oscillations (low frequency modes), and high order IMFs represent fast oscillations (high frequency modes).

EMD- and VMD-based denoising methods require a criterion to separate noise from signal (Li et al., 2015; Liu et al., 2016). Ideally, the decomposed IMFs contain most of the signal while the residual contain most of the noise. Peng et al. (1994) proposed detrended fluctuation analysis (DFA) to analyze different signal trends of unknown duration. They then use scaling exponent estimated from DFA to evaluate the variation of the average root mean square (RMS) fluctuation around the local trend. In addition, the scaling exponent value is an indicator of roughness: the larger the value, the smoother the time series or the slower the fluctuations (Berthouze and Farmer, 2012). Chen et al. (2002) applied DFA on complex noisy signals with varying local characteristics and investigated the strategies for non-stationary signal analysis.

In this paper, we propose a hybrid denoising method combining the DFA and VMD algorithms. We first introduce the principles of EMD and VMD. Using synthetic noisy signal decomposition examples, we evaluate the two algorithms for high and low SNRs. Next, we use the DFA scaling exponents to construct a threshold that excludes noise components. We demonstrate the effectiveness of our workflow through application to a legacy, low fold, land data volume acquired over a limestone play in North Central Texas .

THEORY

VMD vs. EMD

To suppress noise, almost all filtering techniques attempt to differentiate the signal components from the noise components from measured data in either the time or ”transform” domain. EMD adaptively decomposes a multicomponent signal into a finite set of IMFs in the time domain (Huang et al., 1998; Gan et al., 2014). In EMD, IMF components are the mean value of upper and lower envelopes interpolated from the local maxima and local minima of the original signal. The residual obtained by subtracting the original signal and the summation of the acquired IMFs is considered to be a new signal that will be analyzed in the next iteration. EMD stops when the residual satisfies a user-defined stopping criterion. We see EMD as a sifting process with the following representation:

$$s(t)=\sum_{k=1}^{K} IMF_k(t)+r_K(t), \tag{1}$$

where $IMF_k(t)$ is the kth IMF of the signal, and $r_K(t)$ stands for the residual trend.

Dragomiretskiy and Zosso (2014) proposed VMD to decompose intrinsic modes in the frequency domain, which are compact around their respective central frequencies. In VMD, the IMFs are defined as elementary amplitude/frequency modulated (AM-FM) harmonics to model the non-stationarity of the data. In other words, for a sufficiently long interval, the mode can be considered to be a pure harmonic signal. The VMD is realized by solving the following optimization problem:

$$\min_{\{u_k,\omega_k\}} \left\{ \sum_k \left\| \partial_t \left[\left(\delta(t)+\frac{j}{\pi t} \right) * u_k(t) \right] e^{-j\omega_k t} \right\|_2^2 \right\} \quad s.t. \quad \sum_k u_k = d(t), \tag{2}$$

where u_k and ω_k are modes and their central frequencies, respectively. $\delta(\bullet)$ is a Dirac impulse. $d(t)$ is the signal to be decomposed, with the constraint that the summation over all modes should be the input signal. $\left(\delta(t)+\frac{j}{\pi t}\right)*u_k(t)$ indicates the original data and its Hilbert transform.

Figure 1a shows a synthetic 50 Hz signal, and Figure 1b shows its corresponding spectrum. With 3 dB noise (power ratio between signal and noise (PSNR) is about 2) added, the signal becomes noisy. We display noisy signal and noise component in Figures 1c and 1d, with the corresponding spectra in Figures 1d and 1f, respectively.

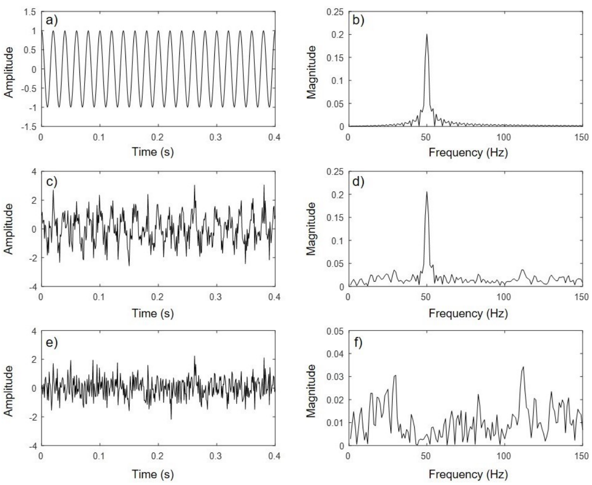

Figure 1: Noisy signal synthetic example: (a) 50 Hz noise free signal with its spectrum (b); (c) 3 dB noisy signal with its spectrum (d); (e) the added noise and the noises spectrum (f).

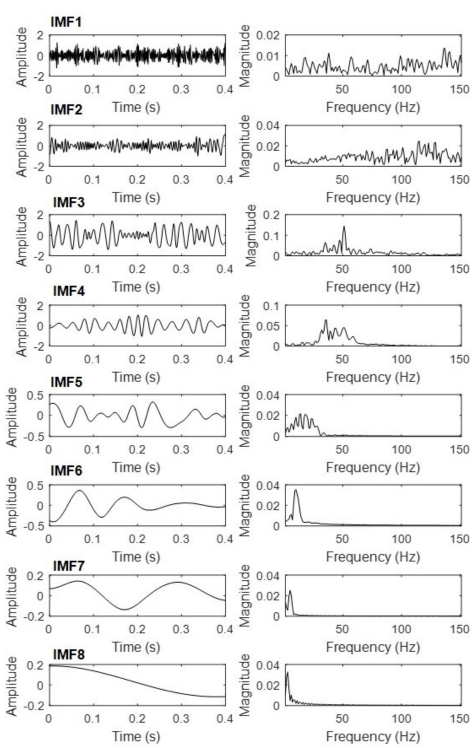

Figure 2: IMF_s from EMD and their corresponding spectra.

Figure 2 demonstrates the decomposed IMFs from EMD and their corresponding spectra, while Figure 3 shows the corresponding products from VMD. Because the number of IMFs produced from EMD is not user-defined, we set the output number of VMD to be the same as that from EMD. Although we truncated the VMD series, VMD better isolates frequency components according to spectra, because of VMDs formulation as an optimization problem in the frequency domain. In particular, the IMF2 component from VMD in Figure 3 closely approximates the original noise free signal. In contrast, none of the results from EMD approximates the signal well.

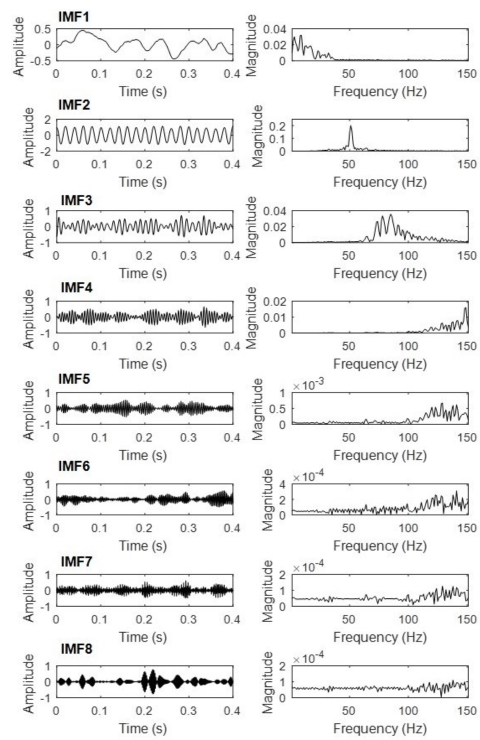

Figure 3: IMF_s from VMD and their corresponding spectra.

A Thresholded VMD Denoising Method

Peng et al. (1994) proposed to use DFA to estimate signal nonstationary properties based on its scaling exponent. If the data (length N) are long-range power-law correlated, the RMS fluctuation around the local trend in the box size n increases following a power law:

$$F(n)=\sqrt{\frac{1}{N}\sum_{k=1}^{K}\left[y(k)-y_n(k)\right]^2} \qquad \propto \qquad n^{\alpha}, \tag{3}$$

where the scaling exponent α is defined as the slope of the curve $[F(n)]/log(n)$, which is estimated as the log-log scale Hurst exponent. $y(k)$ is the time series subtracted from the mean value. $y_n(k)$ is the estimated local trend by simply fitting a linear line. When $0<\alpha<0.5$, the signal is anti-correlated. When $\alpha=0.5$, it corresponds to uncorrelated white noise (Mert and Akan, 2014).

Figure 4 illustrates the proposed denoising workflow. We use VMD to decompose the signal, and DFA to determine the number of IMFs from VMD, as well as the threshold for every IMF in the reconstruction process. In the end, we obtain the filtered signal by summing the first K IMFs with larger α values.

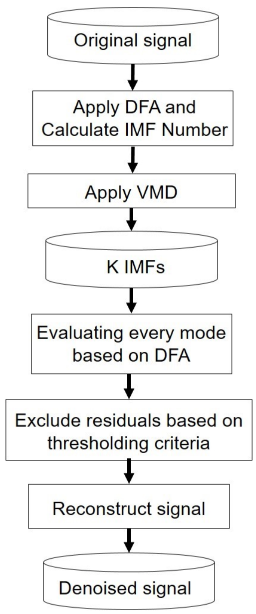

Figure 4: Workflow of the proposed thresholded VMD denoising method.

SINGLE TRACE FILTERING APPLICATIONS

First, we adopt the HeaviSine signal as a synthetic example, we evaluate our algorithm for a suite of different SNRs: 10 dB (PSNR 10), 3 dB (PSNR 2), 0 dB (PSNR 1) and -3 dB (PSNR 0.5). Figure 5 shows filtered results from the proposed method. Note that it performs well even at low SNR cases.

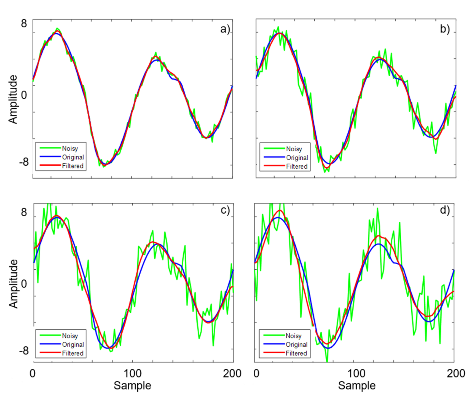

Figure 5: Synthetic example on HeaviSine signal using the proposed denoising approach at different SNR situations: (a) 10 dB, (b) 3 dB, (c) 0 dB, and (d) -3 dB.

Second, we employ a field seismic trace in Figure 6. We also add different levels of noises as the previous example. Again, the VMD-based filter shows stable performance even at low SNR situations, shown in Figure 6.

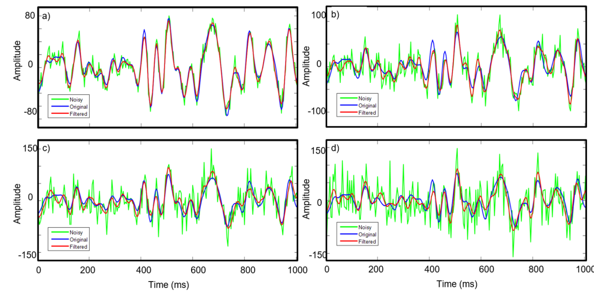

Figure 6: Filtering results on a real seismic signal at different SNR situations: (a) 10 dB, (b) 3 dB, (c) 0 dB and (d) -3 dB.

FIELD APPLICATIONS

In Figure 7, we apply the proposed workflow to a low fold, land seismic survey acquired in the mid-1990s that suffers from backscattered ground roll and migration operator aliasing. This data set is from North Central Texas, here the target is discontinuous high porosity Mississippian Chert (Verma et al., 2016). Figure 7a shows the original seismic data. Figure 7b shows the filtered result, where one notes that both amplitude and phase of the coherent reflectors have been preserved. As a quality control, Figure 7c shows the residual, r_K, (or difference between Figures 7a and 7b) plotted at the same amplitude scale. Laterally continuous events are modeled and steeply dipping coherent noise is rejected. Figure 8 shows the time slice comparison between original data and filtered result. We also calculate the coherence attribute before and after filtering. In Figure 9, note that the discontinuities from noise have been suppressed, and the true geology is preserved.

CONCLUSIONS

We propose a DFA thresholding for VMD based denoising method. A few IMFs of a noisy measured data can represent signal, while the residuals represent noise. To achieve this objective, we use exponents from DFA as a metric to determine which IMFs are noisy oscillations and should be excluded in the reconstruction process. Synthetic and field examples demonstrate that the denoising performance of the proposed method is promising especially at low SNR values.

ACKNOWLEDGMENTS

We thank the industry sponsors of the Attribute-Assisted Seismic Processing and Interpretation (AASPI) Consortium at the University of Oklahoma for their financial support.

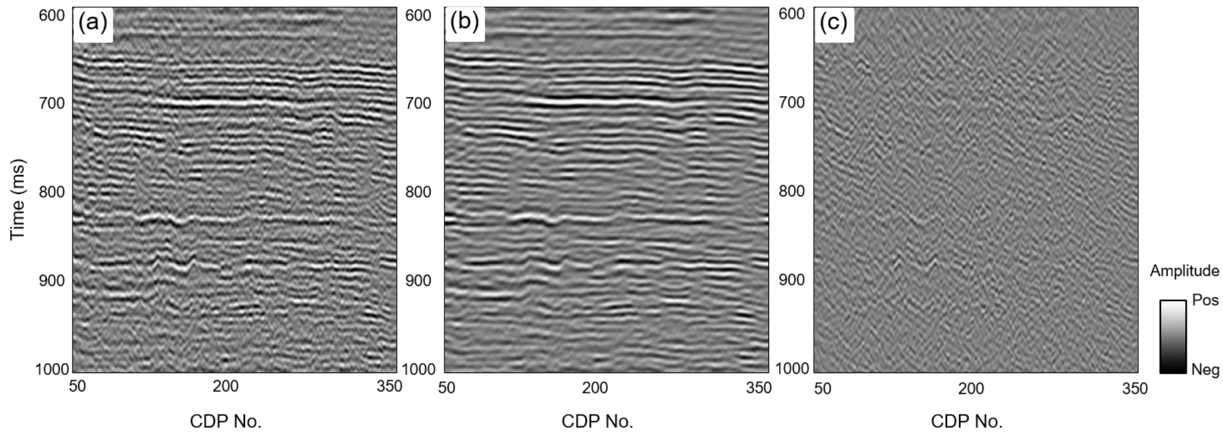

Figure 7: Vertical sections through (a) noisy seismic data, (b) filtered result and (c) difference between noisy data and filtered result. All images plotted using the same amplitude scale.

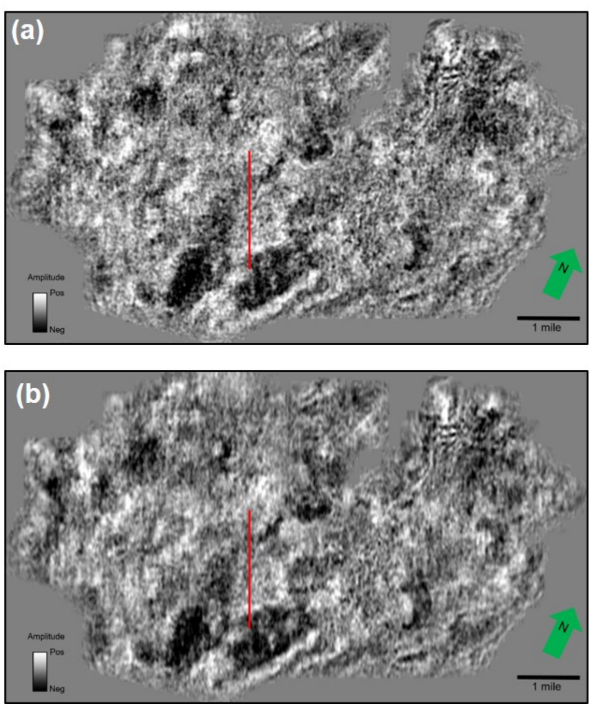

Figure 8: Time slices at t=820 ms through (a) original seismic data and (b) filtered result. It is obvious that the filtered result is smoother.

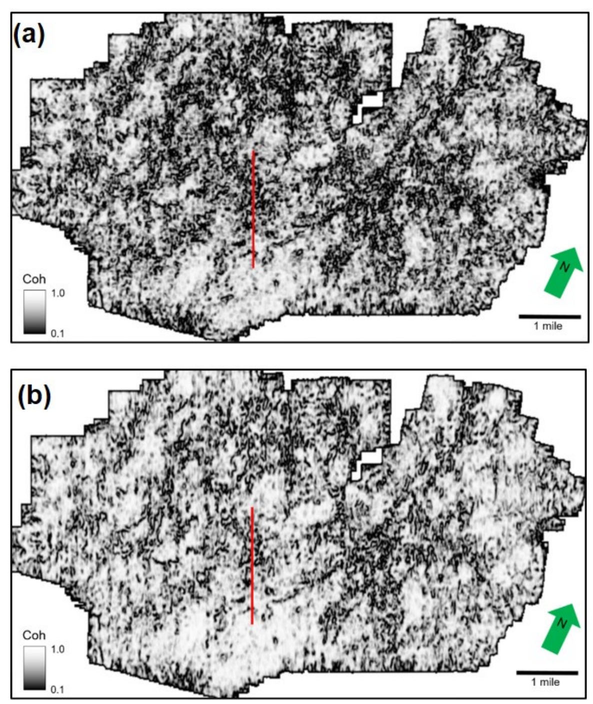

Figure 9: Coherence attribute results of (a) original seismic data and (b) filtered result. Note that less noise interference makes the attribute clearer.

REFERENCES

Berthouze, L., and S. F. Farmer, 2012, Adaptive time-varying detrended fluctuation analysis: Journal of neuroscience methods, **209**, 178–188.

Chen, Z., P. C. Ivanov, K. Hu, and H. E. Stanley, 2002, Effect of nonstationarities on detrended fluctuation analysis: Physical Review E, **65**, 041107.

Chkeir, A., C. Marque, J. Terrien, and B. Karlsson, 2010, Denoising electrohysterogram via empirical mode decomposition: PSSNIP Biosig. And Biorobot. Conf, 32–35.

Donoho, D. L., and I. M. Johnstone, 1994, Ideal spatial adaptation by wavelet shrinkage: biometrika, 425–455.

Dragomiretskiy, K., and D. Zosso, 2014, Variational mode decomposition: IEEE transactions on signal processing, **62**, 531–544.

Gan, Y., L. Sui, J. Wu, B. Wang, Q. Zhang, and G. Xiao, 2014, An emd threshold de-noising method for inertial sensors: Measurement, **49**, 34–41.

Huang, N. E., Z. Shen, S. R. Long, M. C. Wu, H. H. Shih, Q. Zheng, N.-C. Yen, C. C. Tung, and H. H. Liu, 1998, The empirical mode decomposition and the hilbert spectrum for nonlinear and non-stationary time series analysis: Proceedings of the Royal Society of London A: Mathematical, Physical and Engineering Sciences, The Royal Society, 903–995.

Kabir, M. A., and C. Shahnaz, 2012, Denoising of ecg signals based on noise reduction algorithms in emd and wavelet domains: Biomedical Signal Processing and Control, **7**, 481–489.

Li, C., L. Zhan, and L. Shen, 2015, Friction signal denoising using complete ensemble emd with adaptive noise and mutual information: Entropy, **17**, 5965–5979.

Li, F., B. Zhang, K. J. Marfurt, and I. Hall, 2014, Random noise suppression using normalized convolution filter, *in* SEG Technical Program Expanded Abstracts 2014: Society of Exploration Geophysicists, 4345–4349.

Liu, Y., G. Yang, M. Li, and H. Yin, 2016, Variational mode decomposition denoising combined the detrended fluctuation analysis: Signal Processing, **125**, 349–364.

Mert, A., and A. Akan, 2014, Detrended fluctuation thresholding for empirical mode decomposition based denoising: Digital Signal Processing, **32**, 48–56.

Peng, C.-K., S. V. Buldyrev, S. Havlin, M. Simons, H. E. Stanley, and A. L. Goldberger, 1994, Mosaic organization of dna nucleotides: Physical review e, **49**, 1685.

Verma, S., S. Guo, T. Ha, and K. J. Marfurt, 2016, Highly aliased ground-roll suppression using a 3d multiwindow karhunen-loève filter: Application to a legacy mississippi lime survey: Geophysics, **81**, V79–V88.